Latent and Sensible Heat-Transfer Rates in the Boiling of Binary Mixtures

J. R. Thome
Assistant Professor,
Department of Mechanical Engineering,
Michigan State University,
East Lansing, Mich. 48824
Mem. ASME

Nucleate pool boiling bubble departure data were obtained for the liquid nitrogen-argon cryogenic binary mixture system at 1.3 atmospheres absolute pressure. The latent and sensible heat transport rates at individual boiling sites were calculated from the data to deduce their effect on the degradation in the boiling heat-transfer coefficient in binary mixtures. The latent heat-transfer rate is a result of the bubble evaporation mechanism and the sensible heat-transport rate is due to cyclic thermal boundary layer stripping by departing bubbles. The latent and sensible heat-transport rates at individual boiling sites were found to decrease to a minimum at the maximum vapor-liquid mole fraction difference for both constant heat flux and wall superheating conditions. The large decrease in binary boiling heat-transfer coefficients was thus partially explained by the retardation of these two mechanisms and should be included in any model for predicting boiling heat-transfer coefficients in binary and multicomponent mixtures.

Introduction

Nucleate pool boiling of binary mixtures has been a subject of research for a number of years. Research has been directed both at the overall mixture boiling heat-transfer coefficients and, in some cases, also the fundamental aspects of mixture boiling. The present study was done at the fundamental level to ascertain the variation in the latent and sensible heat-transport rates with composition at individual boiling sites in a binary liquid mixture. The binary system of liquid nitrogen and liquid argon was used because of safety considerations and also for their simple molecular shapes. Boiling of cryogenic binary mixtures is of importance to both the air separation and LNG industries.

Hsu and Graham [1] discussed three possible mechanisms which could cause the large heat-transfer coefficients in nucleate pool boiling. These were: (*a*) the bubble agitation mechanism, (*b*) the vapor-liquid exchange mechanism, and (*c*) the evaporation mechanism. The vapor-liquid exchange mechanism and the evaporation mechanism will be considered here to determine the effect a second component has on the sensible heat-transfer rate and the latent heat-transfer rate, respectively.

Several previous studies have investigated the variation in bubble departure size and frequency in binary mixtures: Tolubinskiy and Ostrovskiy [2–4], and Valent and Afgan [5]. The general conclusion of these studies was that the bubble departure diameters decreased to a minimum in the mixtures at about the same composition as the absolute maximum in the mole fraction difference between the vapor and liquid, $|y-x|$. Van Stralen's results, summarized in [6], for boiling from a very thin wire supports this conclusion.

Experimental Equipment and Techniques

Details of the experimental pool boiling cryostat have been previously described elsewhere [7, 8], so only a brief summary is given here.

Boiling took place on a horizontal oxygen-free, high-conductivity (OFHC) copper disk facing upward. The diameter of the disk was 18 mm. Five micro-drilled cavities spaced 2 mm apart were made at the center ranging from 21 to 52 microns in dia with essentially cylindrical shapes. The solder joint adjoining the test surface to its support was carefully polished to retard spurious bubbles from forming and obscurring bubbles growing from the specially prepared sites. The growth cycles of the bubbles from the microdrilled cavities were recorded using a high speed cine camera operating from 500 to 4000 frames per s as the various bubble departure frequencies required.

Measurements of the bubble departure diameters and frequencies from the cine films were obtained manually using an optical comparator at 100× magnification and also with a computerized image analysis system. A description of the latter method has been presented elsewhere [8, 9]. The computerized system was ideal for measuring and storing in computer file large amounts of accurate bubble growth and departure data with relative ease and a minimum of effort. The estimated error in measuring the equivalent bubble departure diameter and frequency were 5 and 2 percent, respectively.

The phase equilibrium data of Thorpe [10] for the nitrogen-argon system were used for the investigation. A summary of the correlating methods for determining the thermodynamic and transport properties of the mixtures can be found in Thome [8]. Table 1 gives the relevant physical properties.

Ultra-high-purity argon gas (99.996 percent) and high-purity nitrogen gas (99.992 percent) were condensed into the test chamber to prepare the test liquids. The gases passed through a liquid nitrogen cold trap prior to entering the cryostat in order to freeze out the remaining water vapor and CO_2 impurities. Using the phase equilibria data of Thorpe [10], the measured saturation pressure and temperature were utilized to determine the test liquid compositions to within ±0.015 mole fraction.

Experimental Bubble Departure Results

Two types of experimental procedures were performed for studying bubble departure: (*a*) constant composition with varying wall superheat and (*b*) constant wall heat flux with varying composition. These were all performed during a single cooldown to cryogenic temperatures. The boiling curves can be found in Thome [8].

The vapor generation rate at an individual boiling site is the product of the bubble departure volume, V_d, and the bubble

Contributed by the Heat Transfer Division and presented at the 20th ASME/AIChE National Heat Transfer Conference, Milwaukee, Wisconsin, August 2-5, 1981. Manuscript received by the Heat Transfer Division September 18, 1981. Paper No. 81-HT-28.

Table 1 Physical properties of Nitrogen-Argon at 1.3 Atm

x (N_2)	y (N_2)	T_{sat} (K)	ρ_L (kg/m^3)	ρ_v (kg/m^3)	h_{fg} (kJ/kg)	c_p (kJ/kgK)	k_L (W/mK)	σ (dyn/cm)
0.0	0.000	89.90	1375	7.35	161	1.14	0.121	11.88
0.1	0.265	87.94	1311	7.46	165	1.18	0.123	11.59
0.2	0.438	86.35	1248	7.32	168	1.23	0.124	11.30
0.3	0.570	85.05	1187	7.15	171	1.29	0.125	11.02
0.4	0.668	83.96	1126	6.95	175	1.36	0.126	10.72
0.5	0.748	83.03	1067	6.76	178	1.44	0.127	10.42
0.6	0.813	82.23	1009	6.58	181	1.53	0.128	10.09
0.7	0.865	81.53	953	6.39	184	1.64	0.128	9.72
0.8	0.912	80.87	899	6.22	188	1.77	0.129	9.32
0.9	0.958	80.23	846	6.05	192	1.91	0.130	8.87
1.0	1.000	79.63	796	5.88	196	2.08	0.131	8.36

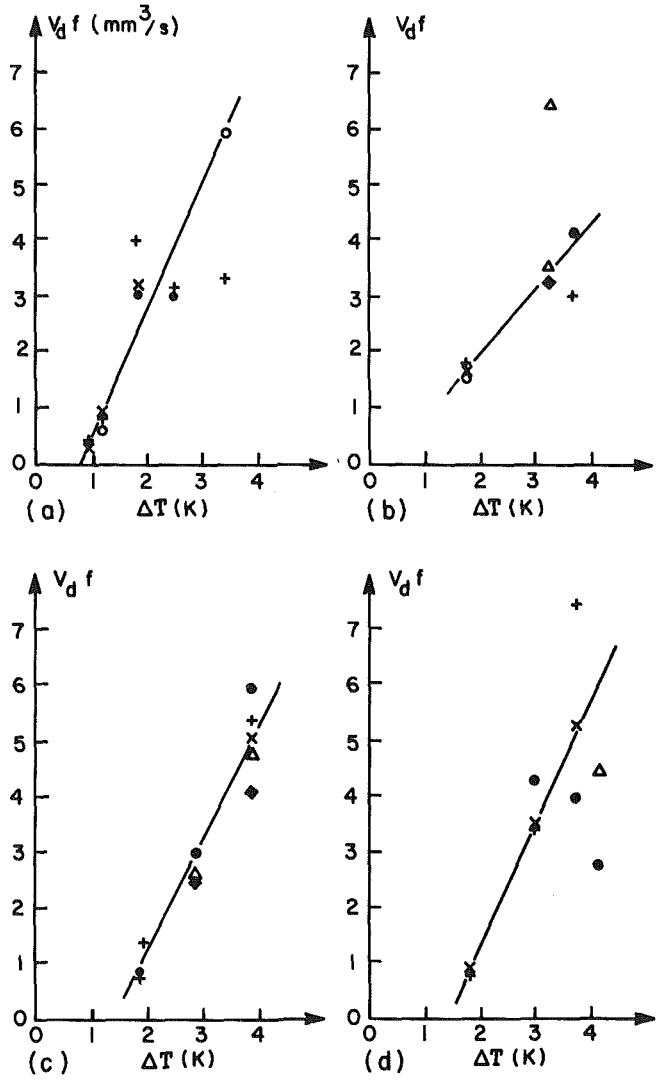

Fig. 1 Variation in vapor generation rate at a boiling site with wall superheat at 1.3 atmospheres pressure: (*a*) nitrogen, (*b*) argon, (*c*) 84 percent mole fraction nitrogen, (*d*) 68 percent mole fraction nitrogen. Legend: x site 1, 52 μm dia; ◆ site 2, 49 μm; • site 3, 40 μm; + site 4, 46 μm; o site 5, 21 μm; ▵ natural sites.

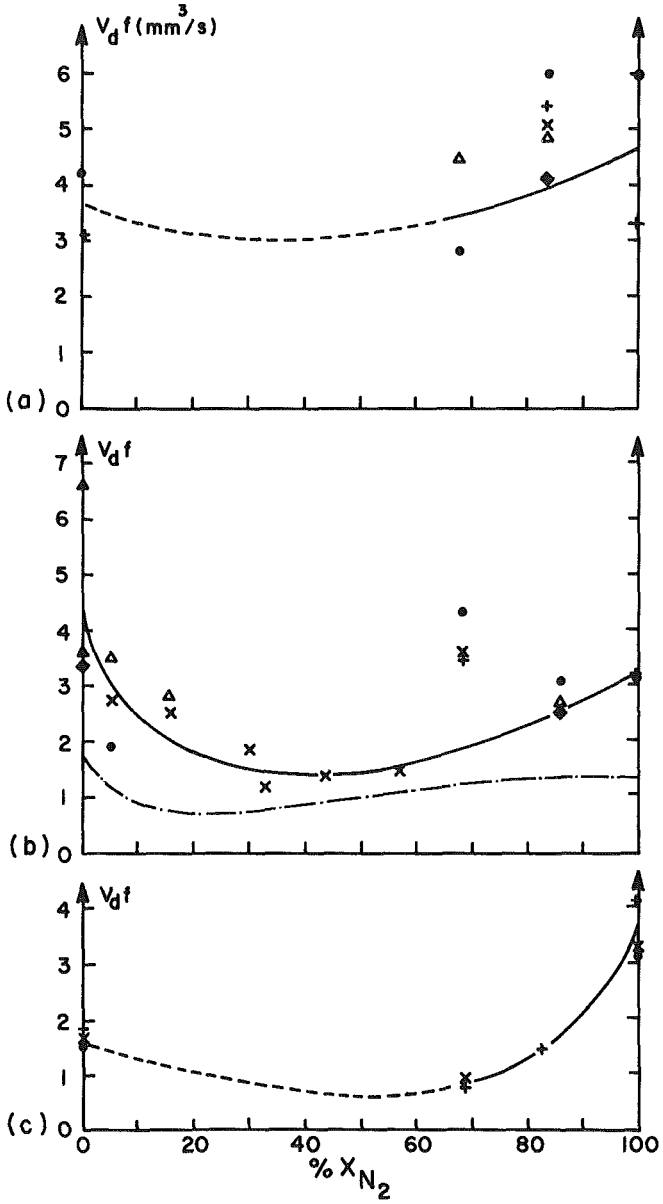

Fig. 2 Variation in vapor generation rate at a boiling site with composition at 1.3 atmospheres pressure and at three heat flux levels: (*a*) 4.3 kW/m^2, (*b*) 2.1 kW/m^2, (*c*) 1.2 kW/m^2. Legend: same as in Fig. 1. The dash/dot/dash line in (*b*) is the theoretical prediction of Thome (*14*).

Nomenclature

c_p = liquid specific heat
D_d = bubble departure diameter
f = bubble departure frequency
h = heat-transfer coefficient
h_{fg} = heat of vaporization
k_L = liquid thermal conductivity
q_{c_p} = sensible heat-transport rate at a boiling site
$q_{h_{fg}}$ = latent heat-transport rate at a boiling site
T_{sat} = saturation temperature
T_w = wall temperature
ΔT = $T_w - T_{sat}$, wall superheat
V_d = bubble departure volume
x = liquid mole fraction
y = vapor mole fraction
ρ_L = liquid density
ρ_v = vapor density

Subscripts

i = ideal
1 = volatile component
2 = nonvolatile component

departure frequency, f. Since the bubble departure volume and frequency tend to vary from one bubble to the next, a sequence of bubble departures was measured at each site and then an average bubble for that site was determined.

The results for the variation of the vapor generation rate, $V_d f$, at individual boiling sites with wall superheat, ΔT, are shown in Fig. 1. The rate of vapor production is seen to increase substantially with a fair amount of scatter among the various boiling sites. The two mixtures with 68 percent and 84 percent nitrogen mole fractions demonstrated this increase in $V_d f$ with superheat with about the same slope as the single components nitrogen and argon. No general trend with respect to cavity diameter was noted. Several natural sites, which happened to be in focus and measurable, have values similar to the values for the artificially made sites. This justifies the usage of artificial sites.

The experimental bubble departure data in Fig. 1(a) compare very favorably with the bubble departure diameters reported by Grigoryev [11] and with the departure diameters and frequencies given by Verkin [12] and Bland [13] for pure liquid nitrogen. No other data appears to be available for liquid argon.

The change in the vaporization rate at a boiling site with composition is shown in Fig. 2 for three different heat flux levels. The intermediate heat flux of 2.1 kW/m^2 was the one where filming was most successful and hence has the widest range of compositions represented. A definite minimum in the vaporization rate is demonstrated at the heat flux of 2.1 kW/m^2. This minimum corresponds fairly closely to the maximum in $|y-x|$ at 33 percent N_2 shown in Fig. 3 for the nitrogen-argon system at 1.3 atmospheres pressure. These same minima in $V_d f$ are found by combining the bubble departure data of Tolubinskiy and Ostrovskiy [3] for the systems: ethanol-water, ethanol-butanol, ethanol-benzene, and methanol-water.

The vaporization rate, $V_d f$, can be estimated theoretically using the bubble departure diameter and frequency equations for binary liquids of Thome [14]. Using a bubble base dia of 50 μm and assuming that the contact angle is 5 deg and that the bubble waiting time is equal to the bubble growth time, the predicted evaporation rate is compared to the 2.1 kW/m^2 heat-flux data in Figure 2(b). Quantitatively, the predicted values are about 50 percent low. But, if the contact angle (which is only known to be small for cryogens) was instead guessed to be 10 deg, the resulting prediction would be quite satisfactory. Also, from a limited number of values deduced from the raw data in the Appendix in Thome [8], the bubble waiting time in the mixtures tends to be about twice the bubble growth time while for pure nitrogen and pure argon they are of roughly the same duration. Including this phenomena, the theory would predict a more profound minimum than shown in Fig. 2(b) and hence yield better qualitative agreement with the data. In summary, the Thome theory is qualitatively correct but better values for the variation in waiting time and contact angle with composition are needed to do a more rigorous test (the theories presented in [1] for predicting the waiting times were not at all successful).

Latent Heat-Transport Rate at a Boiling Site. The latent heat transport rate at an individual boiling site is determined approximately as

$$q_{h_{fg}} = \rho_V h_{fg} V_d f \tag{1}$$

For a bubble growing in a saturated single component liquid this gives a fairly accurate indication of the latent heat-transport rate. For a bubble growing at a heated wall in a saturated binary mixture, however, there will probably be a slight amount of the nonvolatile component condensing at the top of the bubble. As is well known, the binary liquid at the base of the growing bubble is partially stripped of the volatile

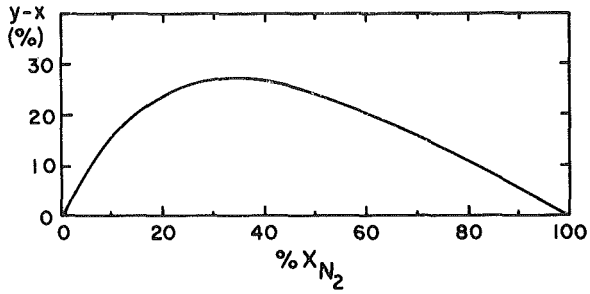

Fig. 3 Vapor-liquid mole fraction difference versus liquid mole fraction of nitrogen for nitrogen-argon system at 1.3 atmospheres

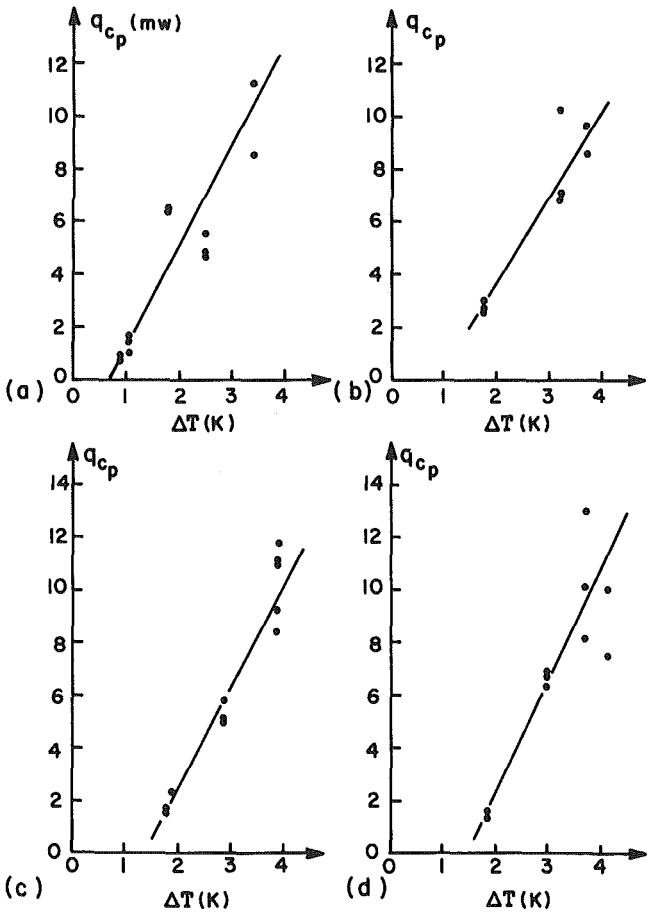

Fig. 4 Change in sensible heat-transport rate at a boiling site with wall superheat: (a) nitrogen, (b) argon, (c) 84 percent nitrogen, (d) 68 percent nitrogen

component (nitrogen) since the vapor mole fraction, y, is greater than the liquid mole fraction, x. Consequently, the local liquid mole fraction at the base of the bubble becomes richer in the nonvolatile component (argon) and more argon is vaporized. However, the top of the bubble is still in contact with the bulk liquid, so the top of the bubble is supersaturated with respect to the nonvolatile component, of which the excess then will tend to condense out. For example, a change in the local saturation temperature of the order of 0.3°C corresponds to a super-saturation of about 3 percent argon in the bubble. If all of this were to condense out, the error in the departure volume would also be on the order of 3 percent, which is within the estimated experimental error in determining V_d. The latent heat-transport rate can still be estimated from equation (1) keeping the above qualification in mind.

Sensible Heat-Transport Rate at a Boiling Site. A number of years ago Forester and Greif [15] proposed a nucleate pool

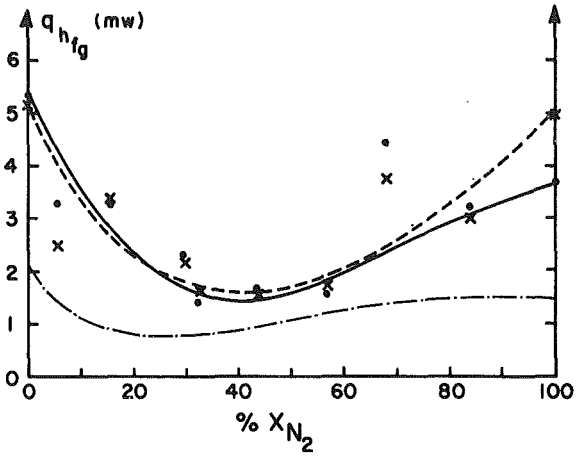

Fig. 5 Variation in the latent heat-transport rate at an average boiling site in the mixtures. Legend: (•) constant heat flux of 2.1 kW/m^2, (x) constant wall superheat of 3.1 K. The dash/dot/dash line is the theoretical prediction of Thome (14).

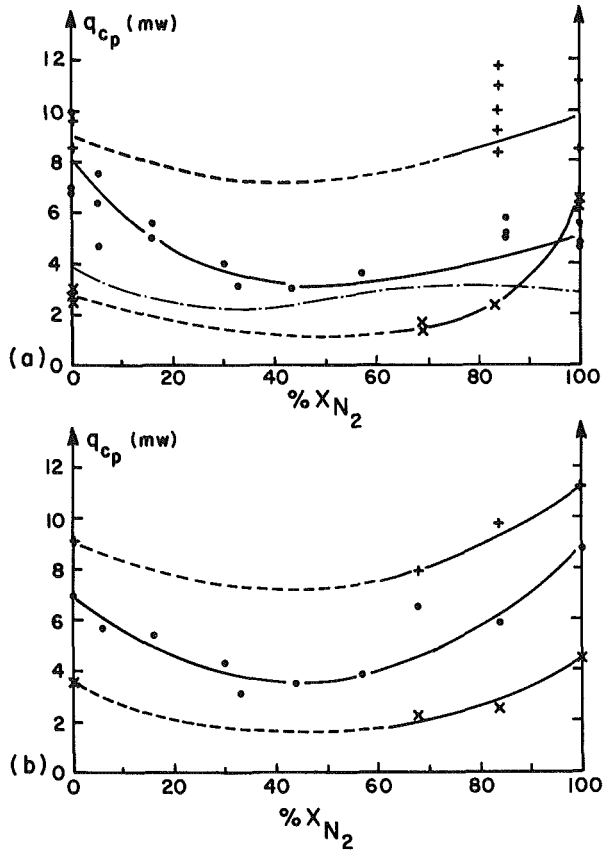

Fig. 6 Variation in the sensible heat-transport rate at a boiling site in the mixtures: (a) constant heat fluxes of 1.2 kW/m^2(x), 2.1 kW/m^2(•), and 4.3 kW/m^2(+), (b) constant wall superheats of 2.0 K(x), 3.1 K(•), and 3.75 K(+). The dash/dot/dash line is the theoretical prediction of Thome.

boiling model for single component liquids based on the vapor-liquid exchange mechanism. They surmized that the thermal boundary layer is cyclically stripped from the heated surface by departing bubbles. They argued that the enthalpy stored in the thermal boundary layer and carried away by a departing bubble is the principal heat-transfer mechanism in boiling. Later, Mikic and Rohsenow [16] developed a similar model and a correlating equation based on this mechanism. Thome [14] has recently extended their model to the nucleate pool boiling of binary mixtures with good agreement to four sets of published boiling data. Basically, the simple model assumes that the volume of hot liquid removed is twice the

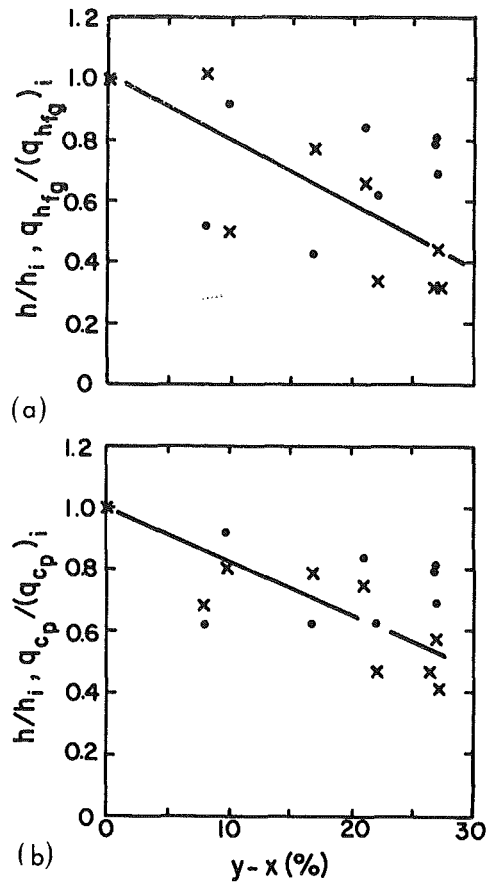

Fig. 7 Comparison of the ratios of the heat-transport rates (x) at an average individual boiling site to the ratio of the overall heat-transfer coefficients (•) for the nitrogen-argon system with a constant wall superheat of 3.1 K: (a) latent heat-transport ratio, (b) sensible heat-transport ratio.

bubble departure diameter in diameter and as thick as the thermal boundary layer. The bubble departure time is used as the characteristic time in calculating the boundary layer thickness from one-dimensional heat conduction to a semiinfinite body. If the average temperature in the boundary layer is also assumed to be ($\Delta T/2$), then the resulting expression for the sensible heat transport rate at a boiling site is:

$$q_{c_p} = \frac{1}{2}\pi^{3/2}(\rho_L c_p k_L f)^{1/2} D_d^2 \Delta T \qquad (2)$$

Variation in Latent and Sensible Heat-Transport Rates with Wall Superheat. Using the nitrogen-argon bubble departure diameters and frequencies, equations (1) and (2) have been evaluated to determine the effect of wall superheat on the latent and sensible heat-transport rates. For the latent heat-transport rates, it is quite evident that these increase exactly the same as $V_d f$ versus ΔT in Fig. 1, but with a multiplying factor of $\rho_v h_{fg}$. The multiplying factors $\rho_v h_{fg}$ for the four cases are: (*a*) 1.15 mJ/mm^3, Nitrogen; (*b*) 1.18, Argon; (*c*) 1.17, 84 percent N_2; and (*d*) 1.19, 68 percent N_2. The overall wall heat fluxes increased about three and a half times from the superheat of about 1.8°C to the highest value on each graph in Fig. 1, and the increases in the latent heat-transport rates are of the same order.

For the sensible heat-transport rates, their variations with wall superheat are shown in Fig. 4. The sensible heat transport rates increased with roughly the same slope for all four compositions.

Variation in Latent and Sensible Heat-Transport Rates with Composition. A large decrease in the latent heat-transport rates in the mixtures compared to the two single component

liquids is demonstrated in Fig. 5. The solid curve is the best fit to the data for a constant wall heat flux of 2.1 kW/m^2. Since the latent heat-transport rate was shown earlier to be a strong function of wall superheat, the data have been interpolated to a wall superheat of 3.1K to illustrate the effect of composition alone. This is depicted by the dashed line. A large decrease with a minimum in the neighborhood of the maximum in $|y-x|$ is again found.

The Thome theory [14] is shown to qualitatively describe the data in Fig. 5 with the previous comments also applying here.

The variation in the sensible heat-transport rate at three constant heat flux levels is depicted in Fig. 6(*a*). As the sensible heat-transport rates in Fig. 6(*a*) are also dependent on wall superheat, the data have again been interpolated to constant wall superheats of 2.0, 3.1, and 3.75 K as shown in Fig. 6(*b*). Thus, a significant decrease in the rate of sensible heat-transport rate in binary mixtures compared to the two single component liquids is evident.

The qualitative agreement between theory and experiment is again evident in Fig. 6(*a*). Quantitative agreement could be enhanced by using a larger contact angle. The slight maximum in q_{c_p} at 70 percent N_2 predicted theoretically is the result of the rise in ΔT here compared to 100 percent N_2, using the boiling curves in [8] for evaluating equation (2) as was done with the other computations.

Comparison to the Variation in the Overall Heat-Transfer Coefficient with Composition. A simple way to compare the change in the boiling heat-transfer coefficient for the whole heated surface to the variation in the latent and sensible heat-transport rates at an individual boiling site is to define the ideal values as

$$\frac{1}{h_i} = \frac{x_1}{h_1} + \frac{x_2}{h_2} \tag{3}$$

$$(q_{h_{fg}})_i = x_1(q_{h_{fg}})_1 + x_2(q_{h_{fg}})_2 \tag{4}$$

$$(q_{c_p})_i = x_1(q_{c_p})_1 + x_2(q_{c_p})_2 \tag{5}$$

where x_1 and x_2 are the mole fractions of the single components one and two in the mixture. Then the ratios of h/h_i, $q_{h_{fg}}/(q_{h_{fg}})_i$, and $q_{c_p}/(q_{c_p})_i$ can be compared by plotting them versus the vapor-liquid composition difference, $(y-x)$.

Figure 7(*a*) shows the comparison between the heat-transfer coefficient ratio and the latent heat-transport ratio. Figure 7(*b*) depicts the comparison of the heat-transfer coefficient ratio to the sensible heat-transport ratio. These comparisons were made at a constant wall superheat of 3.1K to isolate the effect of composition. The general trend is a decrease in the sensible and latent heat-transport rates compared to the ideal mixture values, which is matched by a similar decrease in the heat-transfer coefficient. Thus the effect of mass diffusion controlled bubble growth in a binary mixture is to retard the basic heat-transport mechanisms which in turn reduces the heat-transfer coefficient. A factor not explicitly included here, of course, is the effect of the variation in the boiling site density with composition.

Summary

The following conclusions were reached:

1 The vapor generation rate at an individual boiling site (*a*) increases with superheat in single and two-component liquids and (*b*) decreases to a minimum in the mixtures at the absolute maximum in the vapor-liquid mole fraction difference.

2 The latent and sensible heat-transport rates at an individual boiling site (*a*) increase with superheat in single and two-component liquids and (*b*) decrease to a minimum in the mixtures at the maximum in $|y-x|$.

3 The decrease in the boiling heat-transfer coefficient in binary mixtures can be partially explained by the decrease in the latent and sensible heat transport rates in binary mixtures.

Acknowledgment

The author performed the experimental studies while at the Cryogenics Laboratory, Department of Engineering Science, University of Oxford with the support of the British Science Research Council and the Heat Transfer-Fluid Flow Service of AERE, Harwell, England. The author also wishes to acknowledge the support of the National Science Foundation during the analysis of the experimental work.

References

1 Hsu, Y. Y., and Graham, R. W., *Transport Processes in Boiling and Two-Phase Systems*, McGraw-Hill, Washington, 1976.

2 Tolubinskiy, V., Ostrovskiy, Y. N., and Kriveshko, A. A., "Heat Transfer to Boiling Water-Glycerine Mixtures," *Heat Transfer—Soviet Research*, Vol. 2, No. 1, 1970, pp. 22-24.

3 Tolubinskiy, V. I., and Ostrovskiy, Y. N., "Mechanism for Heat Transfer in Boiling of Binary Mixtures," *Heat Transfer—Soviet Research*, Vol. 1, No. 6, 1969, pp. 6-11.

4 Tolubinskiy, V. I., and Ostrovskiy, Y. N., "On the Mechanisms of Boiling Heat Transfer," *International Journal of Heat and Mass Transfer*, Vol. 9, 1966, pp. 1463-1470.

5 Valent, V., and Afgan, N., "Bubble Growth Rate and Boiling Heat Transfer in Pool Boiling of Ethylalcohol-Water Mixtures," *Warme-und Stoffubertragung*, Vol. 6, 1973, pp. 235-240.

6 Van Stralen, S. J. D. and Cole, R., *Boiling Phenomena*, Vol. 1, McGraw-Hill, New York, 1979.

7 Thome, J. R., and Bald, W. B., "Nucleate Pool Boiling in Cryogenic Binary Mixtures," *Proceedings of the Seventh International Cryogenic Engineering Conference*, IPC Science and Technology Press, London, July 1978, pp. 523-530.

8 Thome, J. R., "Bubble Growth and Nucleate Pool Boiling in Liquid Nitrogen, Argon, and Their Mixtures," D. Phil thesis, University of Oxford, 1978.

9 Preston, G., Thome, J. R., Bald, W. B., and Davey, G., "The Measurement of Growing Bubbles on a Heated Surface Using a Computerized Image Analysis System," *International Journal of Heat and Mass Transfer*, Vol. 22, 1978, pp. 1457-1459.

10 Thorpe, P. L., "Liquid-Vapour Equilibrium of the System Nitrogen-Argon at Pressures up to Ten Atmospheres," *Trans. Faraday Soc.*, Vol. 64, 1968, pp. 2273-2280.

11 Grigoryev, V. A., Pavlov, Yu. M., Ametistov, E. V., and Klimenko, A. V., "Investigation of the Growth Rate of Vapor Bubbles in the Boiling of Cryogenic Fluids," *Heat Transfer—Soviet Research*, Vol. 7, No. 5, 1975, pp. 135-138.

12 Verkin, B. I., and Kirichenko, Yu. A., "Soviet Investigations on Pool Boiling of Cryogenic Liquids," *Proceedings of the Seventh International Cryogenic Engineering Conference*, IPC Science and Technology Press, London, July 1978, pp. 505-522.

13 Bland, M. E., "Bubble Nucleation in Cryogenic Fluids," D. Phil. thesis, University of Oxford, 1970.

14 Thome, J. R., "Nucleate Pool Boiling of Binary Liquids—An Analytical Equation," *AIChE Symposium Series*, No. 208, Vol. 77, 1981, pp. 238-250.

15 Forster, D. E., and Greif, R., "Heat Transfer to a Boiling Liquid: Mechanism and Correlations," ASME JOURNAL OF HEAT TRANSFER, Vol. 81C, No. 1, 1959, pp. 43-46.

16 Mikic, B. B., and Rohsenow, W. M., "A New Correlation of Pool-Boiling Data Including the Effect of Heating Surface Characteristics," ASME JOURNAL OF HEAT TRANSFER, Vol. 81, 1969, pp. 245-250.